

NATIONAL INSTITUTE FOR FUSION SCIENCE

Dynamic Analysis of Compact Helical System Power Supply and Designs of Its Upgrade

S. Tanahashi and S. Yamada

(Received – Aug. 13, 1991)

NIFS-TECH-2

Sep. 1991

RESEARCH REPORT NIFS-TECH Series

This report was prepared as a preprint of work performed as a collaboration research of the National Institute for Fusion Science (NIFS) of Japan. This document is intended for information only and for future publication in a journal after some rearrangements of its contents.

Inquiries about copyright and reproduction should be addressed to the Research Information Center, National Institute for Fusion Science, Nagoya 464-01, Japan.

Dynamic Analysis of Compact Helical System Power Supply
and Designs of Its Upgrade

S. Tanahashi and S. Yamada

National Institute for Fusion Science
Chikusa-ku, Nagoya, 464-01 Japan

Abstract

Computed dynamic waveforms are compared with measured ones for the power supply of the Compact Helical System(CHS) during 1.5T operation and found to be in good agreement.

On the basis of these results, designs for the upgraded power supply for 2T operation are discussed in the two cases, with and without power consumption for additional heating.

In the former case, the additional heating power is supplied from the ac generator that powers the CHS coils.

Electric voltages and currents in the electric circuit are shown for both cases.

These designs show the possibility for 2T operation by addition of some components without changing the ratings of existing components.

Keywords: Compact Helical System, power supply,
dynamic analysis, computer simulation,
Electromagnetic Transient Program,
design.

1. Preface

The Compact Helical System (CHS) [1] and its associated power supply were assembled in March of 1988. This device was designed to generate a magnetic confinement field of up to 1.5 T. A scheme has been developed for increasing the field to a maximum of 2 T for carrying out 112 GHz ECH experiments in order to evaluate prospects for Large Helical Devices (LHD) and compare CHS experimental results with those of the Heliotron-E and ATF.

In this article, we report on a numerical simulation of the existing power supply for the 1.5 T field and compare the obtained results with measured values of its circuit constants; this will be used in computer simulations of basic design variants for upgrading the power supply to increase the field to 2 T. In addition, we studied a variant 2 T power supply in which power for neutral beam injection heating (5.5 MW) and RF heating (5.9 MW) are simultaneously output from a single generator.

We used the EMTP (Electromagnetic Transient Program)[2] in our simulation.

2. CHS Power Supply Overview

The Compact Helical System is made up of a helical field coil (HF), outer vertical field coil (OVF), trimming vertical field coil (TVF), shaping field coil (SF), and inner vertical field coil (IVF). The CHS power supply provides current to all coils via an HF+OVF thyristor rectifier system in series with a 60 MW diode rectifier system supplying the HF and OVF coils, a TVF thyristor rectifier for

the TVF coil, and an SF thyristor rectifier for the SF coil. These components of the CHS power supply are powered by a 125 MVA ac generator [3].

The thyristor power supply for the IVF coil works directly off commercial line voltage, and so falls beyond the scope of this study.

We expected that the generator output voltage for the CHS HF+OV F coils, rated at 3 kV 11 kA for 1.5 T operation, could be set at 1500 V, i.e. 50% of rated value. However, it became apparent during coil excitation tests that this will have to be increased by a factor of from 1.17 to 1.25, depending on test conditions. This difference is due to underestimating the impedance of the 3 MVA transformer in the 60 MW diode rectifier system prior to the test. It will be done to make a more careful estimate of the transformer and rectifier system impedances in this study.

In this article we estimate the impedance of the 60 MW diode rectifier system by using coil excitation test data from the JIPP TII U Tokamak Toroidal Coil powered by a 125 MVA ac generator.

3. Diode Rectifier System Impedances

The 60 MW diode rectifier system is composed of four 3 MVA transformers and four 15 MW rectifiers. The ratings for these components are displayed in Table 1.

The impedance drop over the 3 MVA transformers is 5.09%, or 35% terms of duty-cycle rating (continuous operation equalling 700%), which produces a large voltage drop. Consequently, the values for the resistive and reactive components of the impedance need to be

extremely accurate. Table 2 gives values of the resistance and inductance of the 3 MVA transformers reduced to the secondary (dc) windings.

The 15 MW rectifier is a three-phase bridge-type. Each arm is made up of 500HXD22 silicon diodes in a 3P5S (3 parallel, 5 series) configuration; each 3P has a 10 ohm + 2 microfarad series circuit connected in parallel. The equivalent circuit for an arm as used in the numerical simulation is shown in Fig. 1, with r_1 representing the forward bias over the diodes. Table 3 shows this resistance value as the arm current I_1 is varied. In Fig. 1, L_1 represents the floating inductance of the circuitry.

A 1 microfarad + 60 ohm series circuit is also inserted into the power line going to the 3-phase input of the rectifier.

The 3 MVA transformer impedance is a pivotal value in the numerical simulation of the 60 MW diode rectifier system, so the simulation results need to be checked against JIPP T-IIU coil excitation test data. Comparison of the measured and calculated values in Table 4 show them to be in good agreement.

4. Power Circuitry for CHS 1.5 T Operation

The 125 MVA ac generator has two three-phase stator windings that are magnetically coupled and phase offset, and so the ideal three-phase voltage supply in the equivalent circuit is composed of a reactance and a three-phase delta-Y transformer, as shown in Fig. 2. Here X''_a and X_0 are, respectively, the generator subtransient reactance and the zero-phase inductance; Table 5 gives these values.

Ratings for the 125 MVA ac generator are shown in Table 6.

Fig. 3 is the skelton diagram for the electrical circuit used in the numerical simulation.

The ratings for the transformers in Fig. 3 are adduced in Table 7. The constants for each of the CHS coils (HF+OVF, TVF and SF) and their magnetic coupling vacuum vessels (VV) are shown in Table 8. The HF coil is series-connected to the OVF coil. Current is supplied to this HF+OVF coil via the 60MW diode rectifier system and HF+OVF thyristor rectifier system, with the latter controlling the constant current.

5. Control System for CHS Power Supply During 1.5 T Operation

The 125 MVA ac generator is feedback-controlled to match the output ac voltage waveform at point G in Fig. 3 with that shown in Fig. 4(a). Similarly, the currents in the HF+OVF, SF, and TVF coils are feedback-controlled by their respective thyristors to tailor them into the control target current waveforms shown in Figs. 4(b), 4(c), and 4(d), respectively. The generator voltage setting and control target current value are given numerically in Fig. 4.

6. Comparison of Dynamic Analysis and Coil Excitation Test Results for CHS Power Supply During 1.5 T Operation

The generator voltage setting ($1500V \times 1.17PU = 1755 V$) and HF+OVF, SF, and TVF current settings are those given in Fig. 4. Fig. 5 compares the results of an 8 June 1988 #8 (Mode 2) coil excitation test and calculations obtained from the numerical simulation. In

general, calculated and measured current and voltage waveforms are in good agreement. The calculated coil terminal voltage waveforms in the Figure are low-pass filtered to remove high frequency noise caused by thyristor switching. Except for a few noise-scattered points, the measured and calculated waveforms seem to be in satisfactory agreement.

7. Power Circuitry for Upgrading to 2 T Operation (I)

In the circuit of Fig. 3, increasing the generator out-put voltage to bring the current in the HF+CVF coils up to the 14656 A needed for 2 T operation causes the current to exceed rated values in the 60 MVA diode rectifier system, so we added a 30 MVA diode rectifier in parallel to make it a 90 MVA diode rectifier system. In the numerical simulation, this is equivalent to reducing the 3 MVA rectifier transformer impedance by 2/3 and changing the virtual resistance that simulates diode forward bias to 2.25 milliohms, as shown in Table 3. The virtual transformer equivalent resistance and inductance values for the new 90 MW diode rectifier system are shown in Table 9. Coil constants are shown in Table 10. In the simulation, the current in the HV+OVF coils can reach the needed 14656 A if the 125 MVA ac generator voltage is 2012 V (1.34 PU, where 1 PU = 1500 V) ; the terminal output voltages and currents in this case are shown in Table 11. In this computation we used TVF and SF excitation patterns that maximized apparent power.

It is clear from the calculations that the 125 MVA ac generator output current is never more than 103% of rated current (12.0 kA). Since 3% excess over rated output current is still within the tole-

rance range, 2 T coil excitation is possible by this method. The current and voltage waveforms for this case are shown in Fig. 6.

8. Power Circuitry for Upgrading to 2 T Operation (II)

In this setup, 125 MVA ac generator output voltage is increased to its rated value (3600 V) to supply 11.8 MW (NBI 5.5 MW, RF 6.3 MW) of additional heating power, and two three-phase step-down auto-transformers (SDT1, SDT2) are added to the HF+OVF and SF,TVF systems. The transformer ratings are shown in Table 12, and the skelton diagram for this case in Fig. 7.

8.1 Maximum Thyristor Phase Control Angle

The impedance seen by the power supply side from each thyristor increases if step-down transformers are added, and so to prevent commutation failure during the inverter commutating period, the thyristor phase control angle must be less than or equal to a maximum value α_{max} given by the following formula [4]:

$$\cos \alpha_{max} = 2\omega L I_d / E_m - \cos \gamma$$

Here I_d is the dc current, E_m the power line voltage peak amplitude, ω the angular frequency, L the commutation inductance seen by the rectifier transformer output terminals for each phase (Y), and γ the commutation margin angle. Table 13 shows the total commutation inductance on the secondary side of thyristor rectifier transformers and the corresponding maximum control angles. The commutation margin

angle is assumed to be 30 degrees.

8.2 Numerical Simulation of Power Circuitry for Upgrading to 2 T Operation (II)

The results of numerical simulation of the circuitry for simultaneously increasing output power and supplying additional heating power are shown in Fig. 8. Voltage, current and apparent power at the two terminals of the 125 MVA ac generator stator windings are shown in Table 14. We used the coil excitation mode that maximized apparent power in the SF and TVF systems. It is clear from comparison of this Table and Table 6 that the voltage never exceeds rated voltage by more than 2% at the first output terminal and 3.4% at the second, and so could be safely utilized. We also see by looking at the current and voltage waveforms at the end of excitation in Fig. 8 that there is almost no commutator failure for rapid coil current decays. This was the reason for limiting the control angle to a safe range in section 8.1 of this study.

9. Conclusion

The results of coil excitation tests and numerical simulation of 1.5 T operation of the CHS device were in good agreement. This would seem to confirm the correctness of the various constants used in simulating 2 T operation.

Conclusions from study of the power supply circuitry for 2 T operation of the CHS device are summarized below.

(1) If no additional heating power is required, 2 T operation

is possible by adding new diode rectifier system settings (dc output power of 6 kV, 5 kA).

(2) If additional heating power of 11.8 MW is required, 2 T operation is possible by adding two additional step-down transformers (55 MVA each) and the new rectifier system (dc 6kV, 5kA). In this case, the thyristor control angle range has to be reduced.

In any case, there is no need to alter the rated values of the components in the existing devices.

Acknowledgements

Morihiro Kubo, Yukio Ishigaki, and Shunsaku Kamiya of Hitachi Corp. assisted us with comparison of CHS power supply simulation and coil excitation data, and Toshiya Kai and Midori Ohiuki of Toshiba Corp. assisted with our study of the generator constants. Our sincere thanks go out to them.

References

- [1] K.Nishimura et al., Proc. 15th Symp. on Fusion Technology, Vol.1, p.398(1988)
- [2] H.W.Dommel, Digital Computer Solution of Electromagnetic Transients in Single and Multiphase Networks, IEEE Trans. on Power Apparatus and Systems, Vol.PAS-88, No.4 (1969)
- [3] J.Kodaira, A.Miyahara, K.Matsuura, K.Hirayama, S.Nohara and Y. Hirata, Constant current and constant voltage excitation of large coils by flywheel-generator-converter, Proc.10th Symp. on Fusion Technology, Vol.1, p.989.
- [4] D.G. Fink and D.Christiansen, Electronic Engineers' Handbook, 2nd Edition, p.15-18 (1982), McGraw-Hill, New York

Table 1 Ratings of the components in the 60MW diode rectifier system

	3MVA Transformers		15MW diode rectifiers
	Primary winding	Secondary winding	
Line voltage	3000V	5800V	6000V
Line current	577A	299A	2500A
Operation	2sec./every 5 min.		2sec./ every 5 min.
% impedance drop	%IZ=5.09 %IR=0.763(75°C) %IX=5.02(96Hz)		

Table 2 Resistance and inductance of 3MVA transformers (reduced values to the secondary winding)

$R_{\Delta} = 0.256 \Omega / \text{Phase (Delta)}$
$L_{\Delta} = 2.80 \text{mH} / \text{Phase (Delta)}$

Table 3 Values of the virtual resistance r_1 simulating the forward bias in an arm of the diode bridge at arm current I_1

Operation	Arm current I_1	Virtual resistance r_1
1.5T in CHS	2.75 kA	3.0 m Ω
1 PU in JIPP T-II U	2.5 kA	3.3 m Ω
2T in CHS	3.67 kA	2.25m Ω

Table 4 Comparison of simulation values with measured values for toroidal coil excitation of JIPP T-II U Tokamak

	Output voltage of the generator	Output current of the generator	Terminal voltage of the coil	Coil current
Measured values	2520V	6800A	4965V	9418A
Calculated values	2520V	6807A	5060V	9440A
Difference	—	0.10%	1.9%	0.23%

Table 5 Measured reactances of the 125 MVA ac generator

Items	Reactance	Inductance*
Subtransient reactance X''_d	0.05748 Ω	0.0762 mH
Zero-phase-sequence reactance X_0	0.02934 Ω	0.0389 mH

*calculated from the reactance at a frequency of 120 Hz

Table 6 Ratings of the 125 MVA ac generator

Line voltage	3000 V
Line current	12029 A \times 2
Apparent power	62.5 MVA \times 2
Power-factor	0.8
Frequency	120 Hz

Table 7 Ratings of the transformers

Name	Capacity	Legend	Frequency	Primary voltage	Secondary voltage	Impedance	Equivalent impedance reduced to the secondary windings
HF+OVF transformer	4.6 MVA \times 2	T _{HO}	96-120 Hz	2100V(Δ)	127V(Y) 220V(Δ)	%IZ=12.5 (4.6MVA127V) Z:R=10:2 R=0.263m Ω (Y) X=1.288m Ω (Y)	L=.00205mH(Y) R=0.263m Ω (Y) L=.00615mH(Δ) R=0.789m Ω (Δ) (f=100Hz)
Auto-transformer	10 MVA	T _T	96-120 Hz	2100V(Δ) 1212V(Y) =V ₁ Input tap2 Output tap1	6300V(Δ) 3637V(Y) =V ₂ V ₂ -V ₁ = 2425V(Y)	%IZ=10.1 (10MVA3637V) Z:R=10:2 R=0.080 Ω (Y) X=0.392 Ω (Y)	upper winding L=0.624mH(Y) R=0.080 Ω (Y) (f=100Hz)
SF/TVF transformer	2.70 MVA \times 2	T _{ST}	60Hz	6300V(Δ)	333V(Y) 577V(Δ)	%IZ=3.26 (2.70MVA333V) Z:R=10:2 R=0.803m Ω (Y) X=3.94 m Ω (Y)	L=0.0104mH(Y) R=0.803m Ω (Y) (f=60Hz)

Table 8 Constants of CHS coils and a vacuum vessel for 1.5T operation

	Inductance (mH)					Resistance (mΩ)
	HF	OVF	TVF	SF	VV	
HF	7.2					215
OVF	-9.72	6.72				30
TVF	-14.4	8.70	1.7			62
SF	-9.19	1.94	3.14	8.91		72
VV	0.245	-5.88×10^{-2}	-3.72×10^{-2}	-5.36×10^{-2}	0.18×10^{-2}	1

Table 9 Overall equivalent resistance and inductance of the virtual transformers for the upgraded 90MVA diode rectifier (reduced values to the secondary winding)

$R_{\Delta} = 0.171 \Omega / \text{phase}$ $L_{\Delta} = 1.867 \text{ mH} / \text{phase}$
--

Table 10 Constants of CHS coils and a vacuum vessel for 2T operation

	Inductance (mH)					Resistance (mΩ)
	HF	OVF	TVF	SF	Vacuum vessel	
HF	72					215
OVF	-14.53	14.42				51
TVF	-9.62	9.41	7.6			41
SF	-9.19	2.99	2.10	8.91		72
Vacuum vessel	0.245	-8.78×10^{-2}	-3.9×10^{-2}	-5.36×10^{-2}	1.8×10^{-3}	1

Table 11 Calculated output voltages, currents and apparent powers of the two output terminals of the 125 MVA ac generator for 2T operation (I)

	Output voltages	output currents	Apparent powers
1st output terminal	1959V	12.38KA	42.0MVA
2nd output terminal	1990V	12.38KA	42.7MVA

Table 12 Ratings of the stepdown auto-transformer

Primary voltage	Secondary voltage	Power capacity	Impedance drop	Inductance reduced to the high side winding
3000V	2200V	55MVA	20%	0.0521mH

Table 13 Commutation inductances of the thyristor rectifier and maximum control angles

Rectifier	E_m	I_d	Commutation inductance L	α_{max}
HF+OVF	311V	14.7kA	2.62 μ H	128°
TVF/SF	816V	5.0kA	15.6 μ H	130°

Commutation margin angle $\gamma = 40^\circ$

Table 14 Calculated output voltages, currents and apparent powers of the two output terminals of the generator for 2T operation (II)

	Output voltages	Output currents	Apparent powers
1st output terminal	3,062V	9.546kA	50.6MVA
2nd output terminal	3,111V	9.829KA	53.0MVA

Figure Captions

- Fig. 1 Equivalent circuit of an arm in the three phase diode bridge (15MW rectifier). The value of r_1 is shown in Table 3.
- Fig. 2 Equivalent skelton diagram of the 125MVA ac generator with two three-phase stater windings.
- Fig. 3 Skelton diagram of the power supply system for CHS or JIPP T-II U Tokamak.
- Fig. 4 Reference voltage and currents for 1.5T operation of CHS.
- Fig. 5 Comparison between calculated and measured waveforms of voltages and currents in CHS at 1.5 T operation.
- Fig. 6 Computed waveforms of voltages and currents in 2T operation without stepdown auto-transformers.
- Fig. 7 Skelton diagram of the power supply system with stepdown auto-transformer for 2T operation
- Fig. 8 Computed waveforms of voltages and currents in the 2T operation with stepdown auto-transformers.

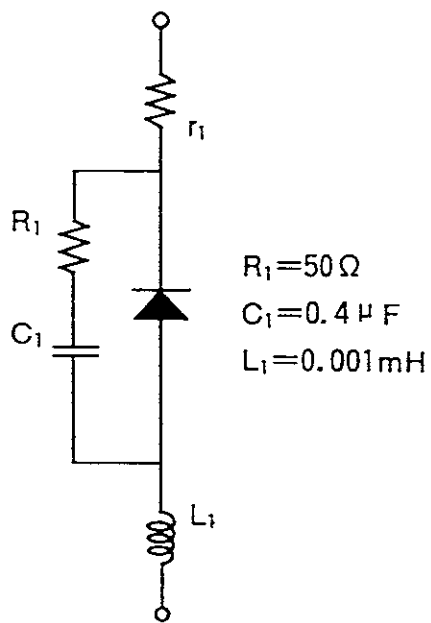


Fig. 1

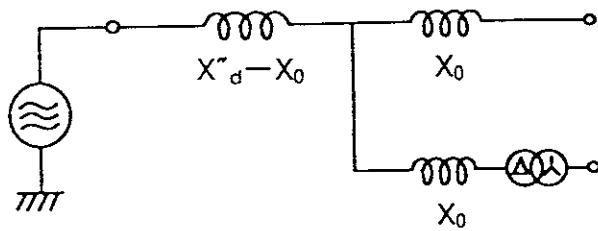


Fig. 2

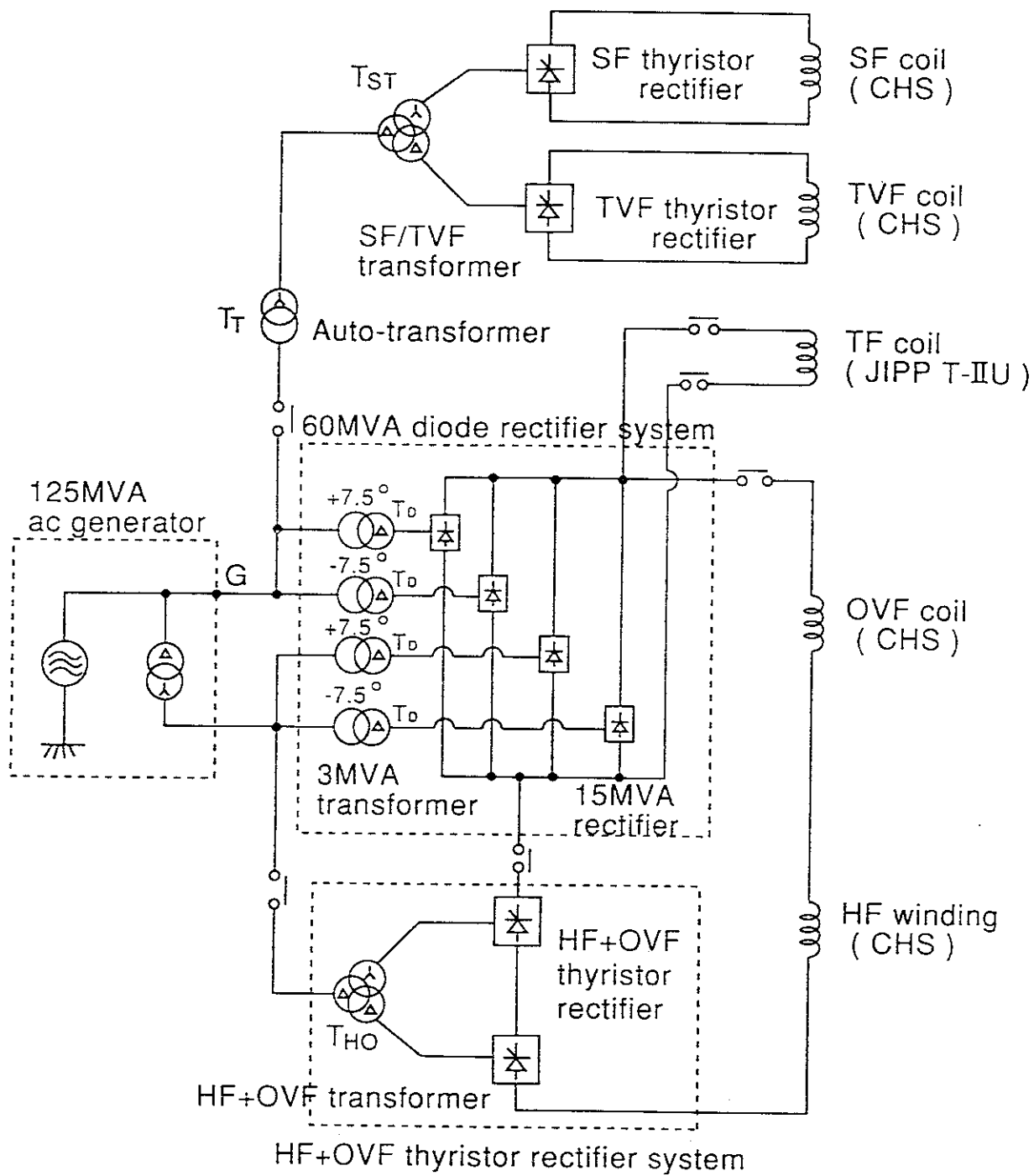


Fig. 3

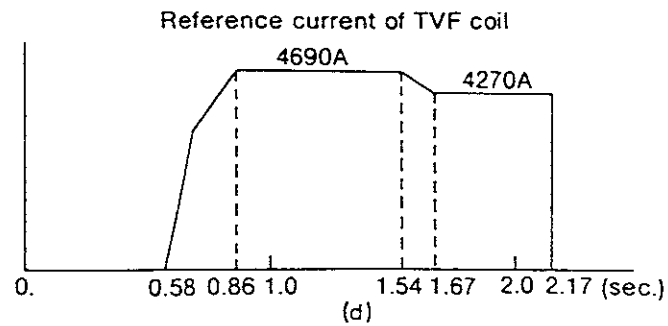
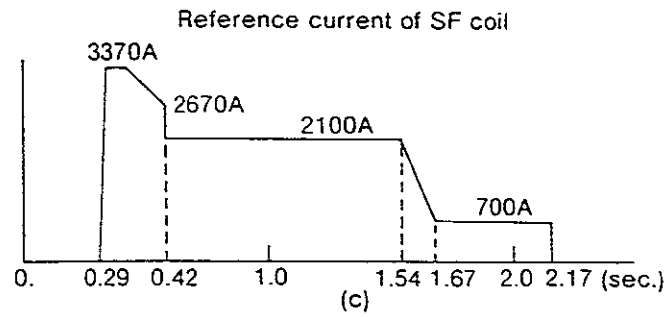
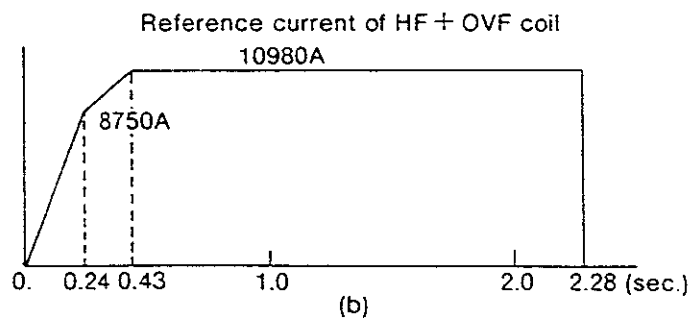
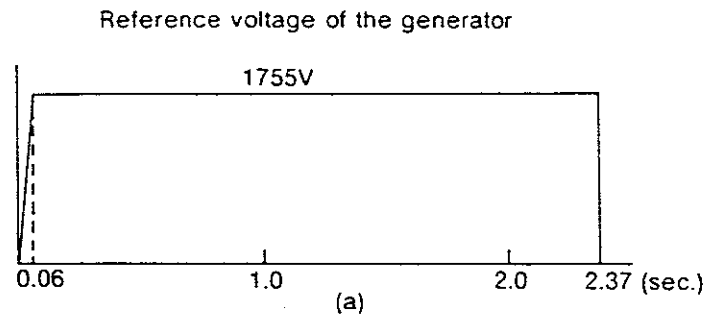


Fig. 4

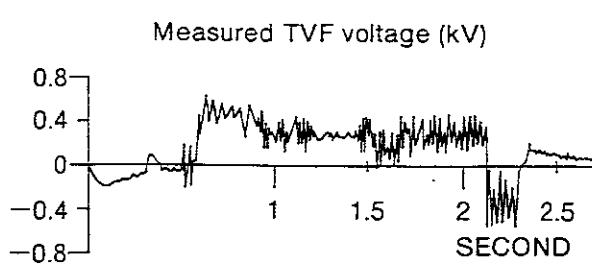
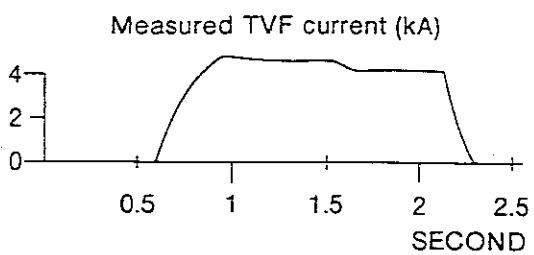
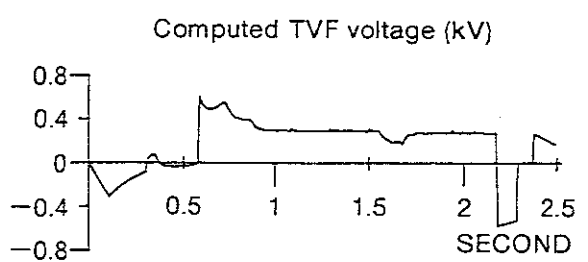
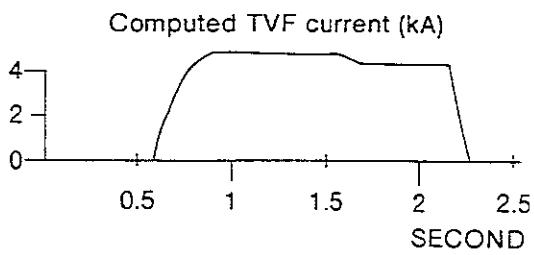
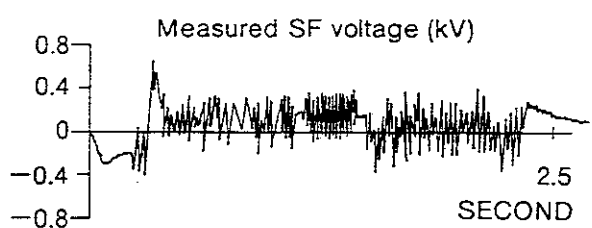
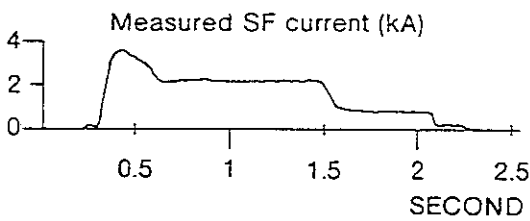
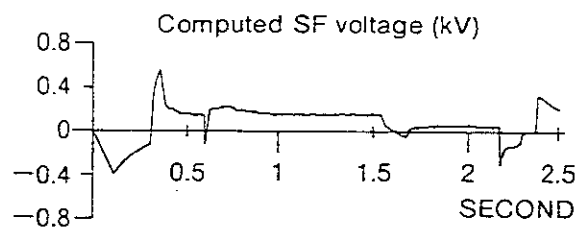
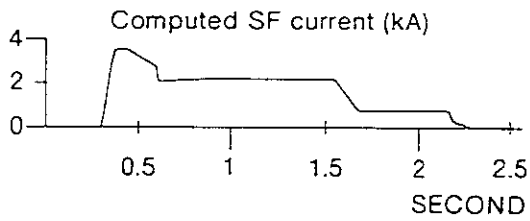
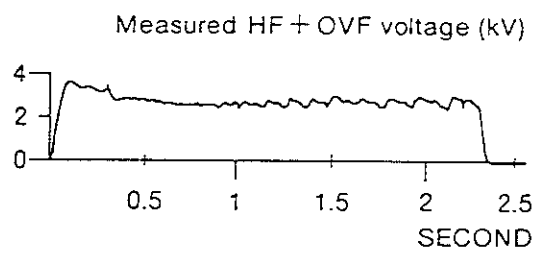
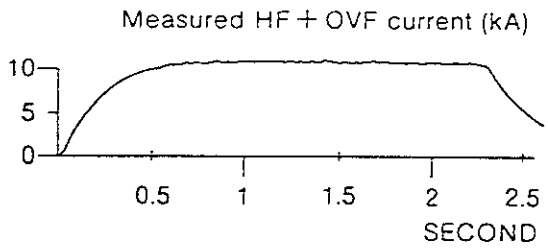
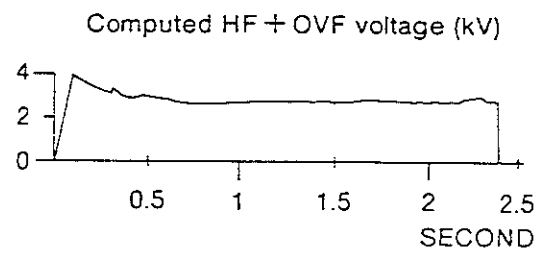
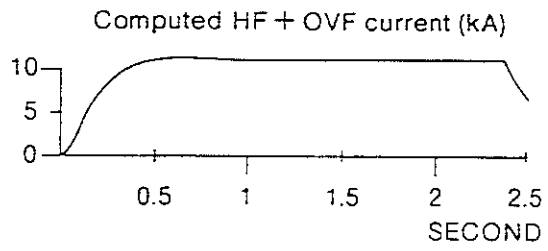


Fig. 5

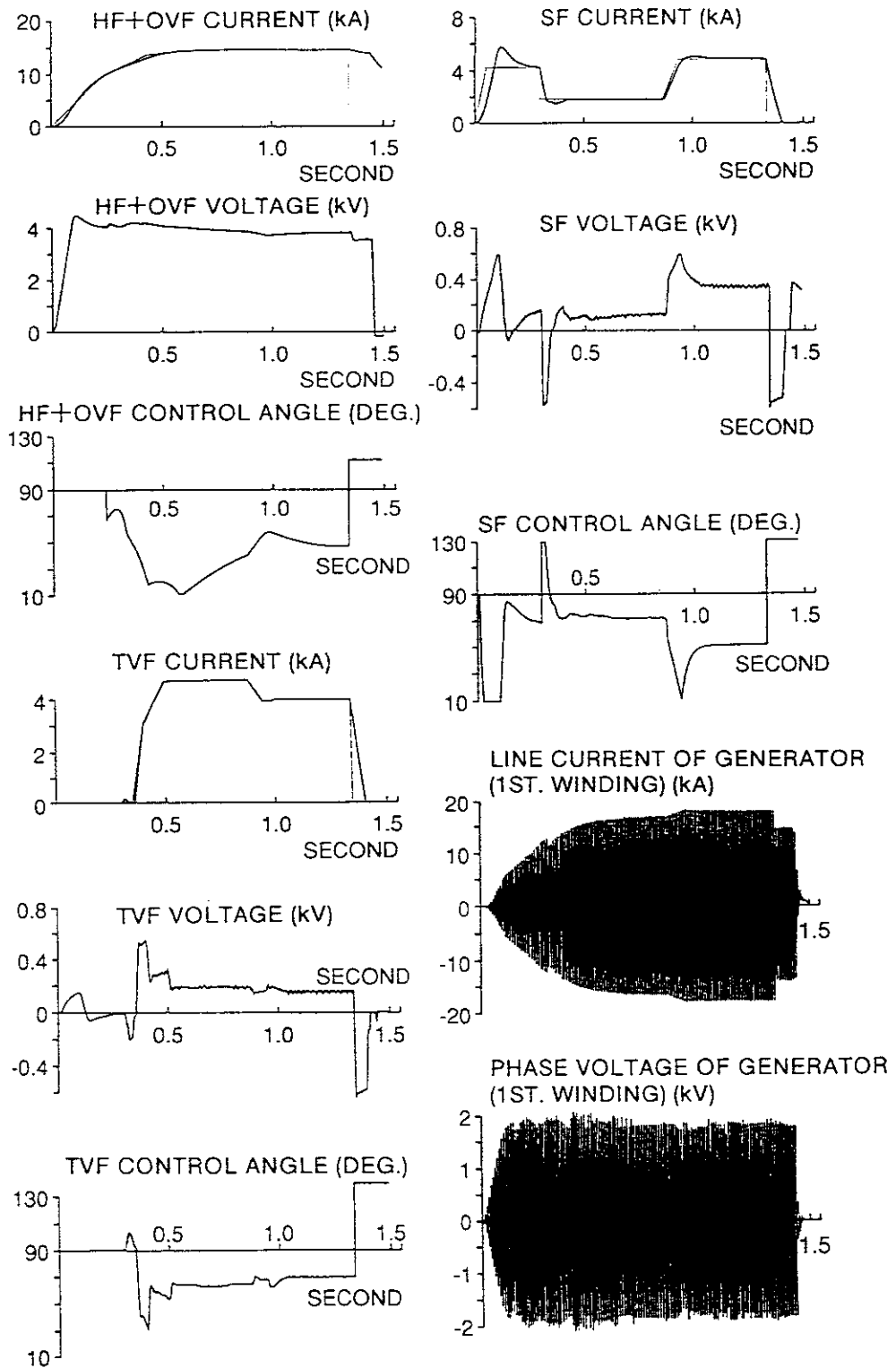


Fig. 6

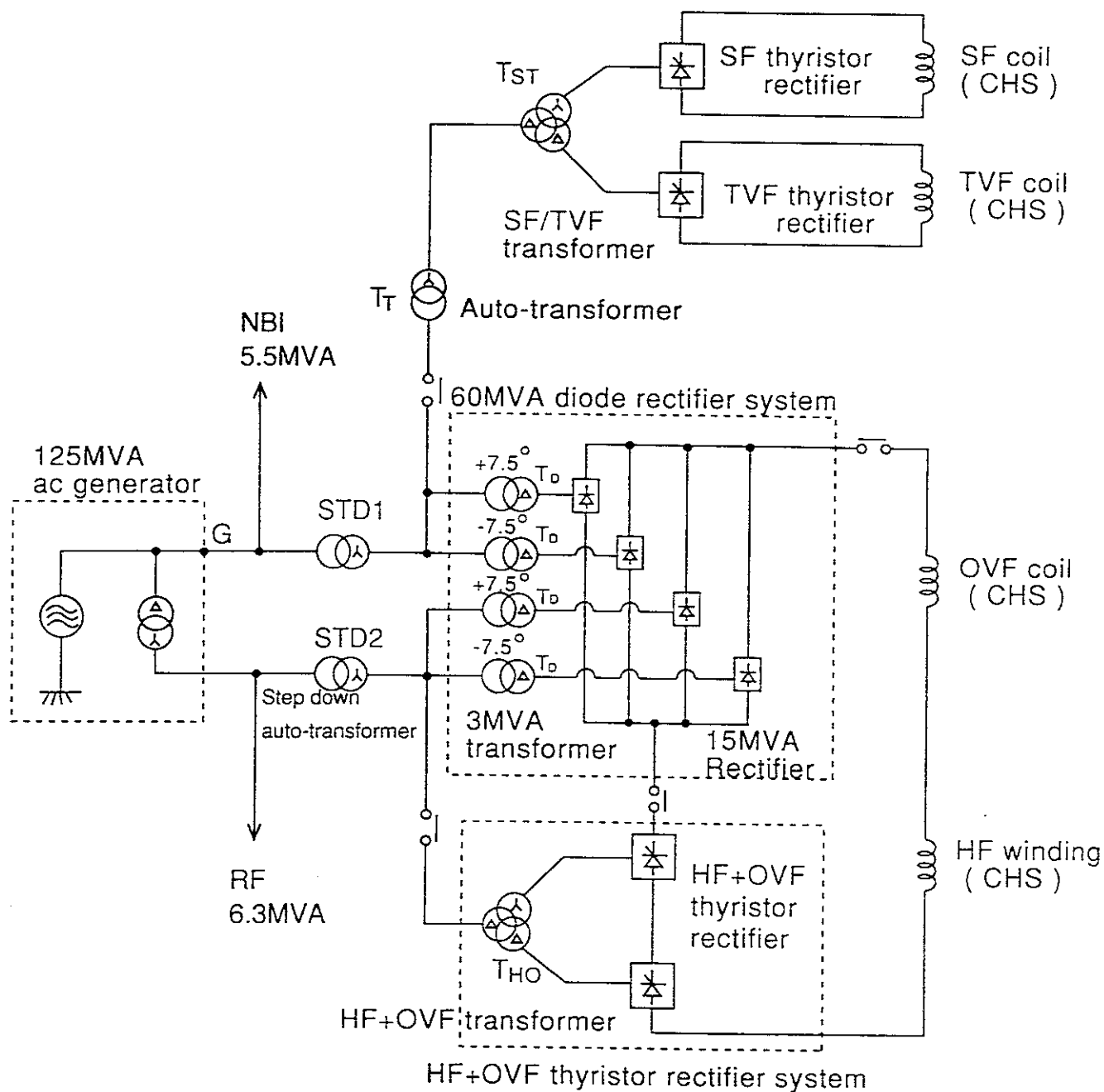


Fig. 7

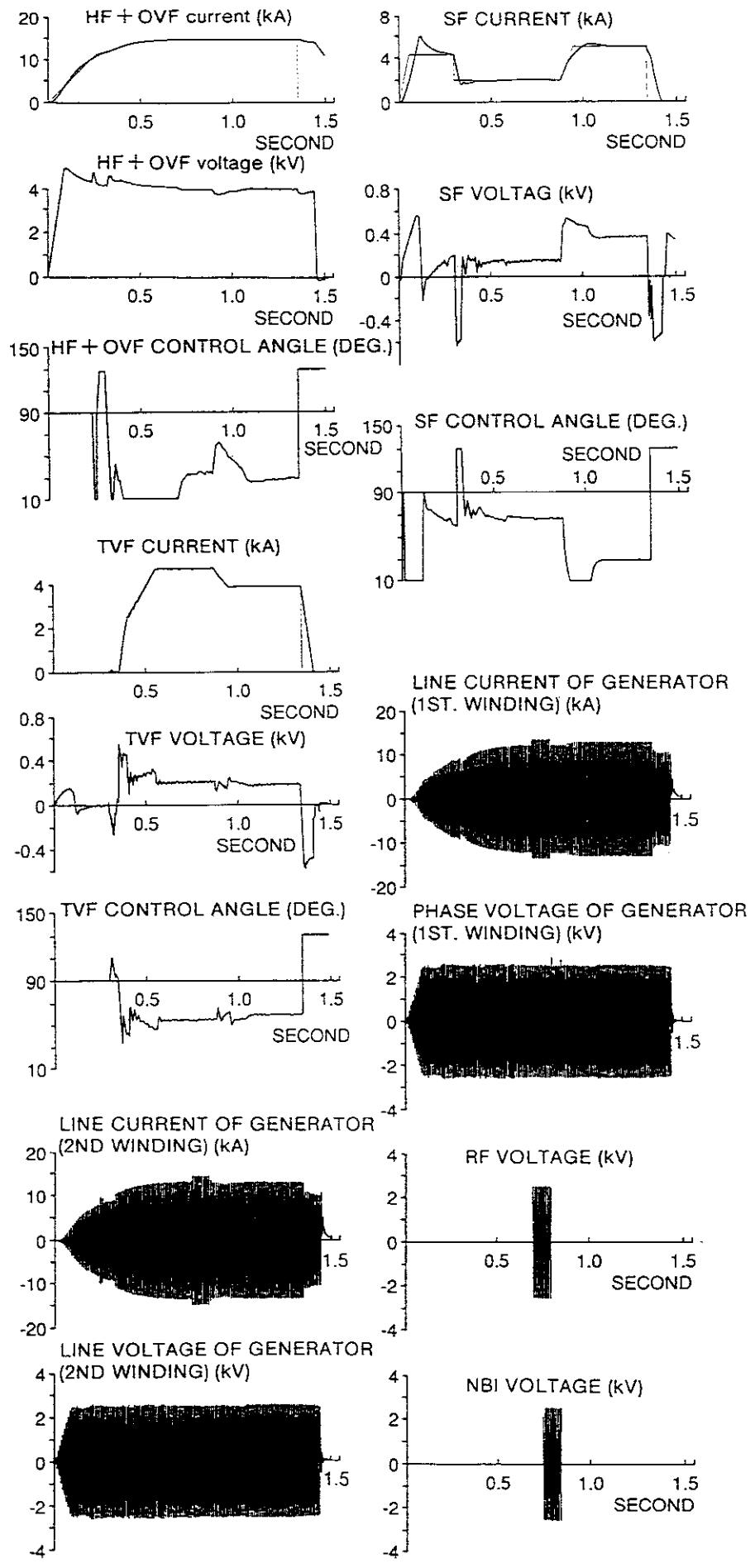


Fig. 8

Recent Issues of NIFS Series

NIFS-TECH-1 H. Bolt and A. Miyahara, *Runaway-Electron -Materials Interaction Studies* ; Mar. 1990